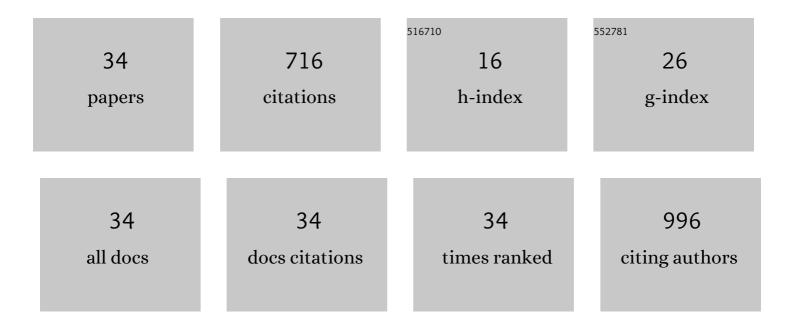
Jin-Long Li

List of Publications by Year in descending order

Source: https://exaly.com/author-pdf/2833271/publications.pdf Version: 2024-02-01



#	Article	IF	CITATIONS
1	Structure and biological properties of mixed-ligand Cu(II) Schiff base complexes as potential anticancer agents. European Journal of Medicinal Chemistry, 2017, 134, 207-217.	5.5	90
2	Bioactive C ₂₁ Steroidal Glycosides from the Roots of <i>Cynanchum otophyllum</i> That Suppress the Seizure-like Locomotor Activity of Zebrafish Caused by Pentylenetetrazole. Journal of Natural Products, 2015, 78, 1548-1555.	3.0	59
3	Highly Efficient Lightâ€Emitting Diodes Based on an Organic Antimony(III) Halide Hybrid. Angewandte Chemie - International Edition, 2022, 61, .	13.8	51
4	Dithiocarbazate-Copper Complexes for Bioimaging and Treatment of Pancreatic Cancer. Journal of Medicinal Chemistry, 2021, 64, 5485-5499.	6.4	49
5	Identification and Evaluation of Antiepileptic Activity of C ₂₁ Steroidal Glycosides from the Roots of <i>Cynanchum wilfordii</i> . Journal of Natural Products, 2016, 79, 89-97.	3.0	40
6	PKA- and Ca2+-dependent p38 MAPK/CREB activation protects against manganese-mediated neuronal apoptosis. Toxicology Letters, 2019, 309, 10-19.	0.8	30
7	Vanadium-oxo immobilized onto Schiff base modified graphene oxide for efficient catalytic oxidation of 5-hydroxymethylfurfural and furfural into maleic anhydride. RSC Advances, 2016, 6, 101277-101282.	3.6	28
8	Antimony, a novel nerve poison, triggers neuronal autophagic death via reactive oxygen species-mediated inhibition of the protein kinase B/mammalian target of rapamycin pathway. International Journal of Biochemistry and Cell Biology, 2019, 114, 105561.	2.8	28
9	Multistage virtual screening and identification of novel HIV-1 protease inhibitors by integrating SVM, shape, pharmacophore and docking methods. European Journal of Medicinal Chemistry, 2015, 101, 409-418.	5.5	27
10	JNK activation-mediated nuclear SIRT1 protein suppression contributes to silica nanoparticle-induced pulmonary damage via p53 acetylation and cytoplasmic localisation. Toxicology, 2019, 423, 42-53.	4.2	27
11	PTP1B inhibitors from stems of Angelica keiskei (Ashitaba). Bioorganic and Medicinal Chemistry Letters, 2015, 25, 2028-2032.	2.2	23
12	Promotion of SIRT1 protein degradation and lower SIRT1 gene expression via reactive oxygen species is involved in Sb-induced apoptosis in BEAS-2b cells. Toxicology Letters, 2018, 296, 73-81.	0.8	21
13	p62/SQSTM1 accumulation due to degradation inhibition and transcriptional activation plays a critical role in silica nanoparticle-induced airway inflammation via NF-κB activation. Journal of Nanobiotechnology, 2020, 18, 77.	9.1	21
14	Obtaining a high value branched bio-alkane from biomass-derived levulinic acid using RANEY® as hydrodeoxygenation catalyst. RSC Advances, 2016, 6, 93956-93962.	3.6	20
15	Endosomal/lysosomal location of organically modified silica nanoparticles following caveolae-mediated endocytosis. RSC Advances, 2019, 9, 13855-13862.	3.6	19
16	Akt inhibition-dependent downregulation of the Wnt/β-Catenin Signaling pathway contributes to antimony-induced neurotoxicity. Science of the Total Environment, 2020, 737, 140252.	8.0	18
17	Dual anti-ischemic effects of rosmarinic acid n-butyl ester via alleviation of DAPK-p53-mediated neuronal damage and microglial inflammation. Acta Pharmacologica Sinica, 2017, 38, 459-468.	6.1	16
18	Potential hypoglycemic effect of acetophenones from the root bark of <i>Cynanchum wilfordii</i> . Natural Product Research, 2019, 33, 2314-2321.	1.8	16

Jin-Long Li

#	Article	IF	CITATIONS
19	Circularly Polarized Luminescence based on 0D Leadâ€Free Antimony (III) Halide Hybrids. Advanced Optical Materials, 2022, 10, .	7.3	16
20	UV–O ₃ treated annealing-free cerium oxide as electron transport layers in flexible planar perovskite solar cells. Nanoscale Advances, 2020, 2, 4062-4069.	4.6	15
21	Two new humulanolides from the roots of Cynanchum wilfordii. Tetrahedron Letters, 2015, 56, 6503-6505.	1.4	14
22	Effects of Geniposide from Gardenia Fruit Pomace on Skeletal-Muscle Fibrosis. Journal of Agricultural and Food Chemistry, 2018, 66, 5802-5811.	5.2	14
23	Benzoic Acid/TEMPO as a Highly Efficient Metalâ€Free Catalyst System for Selective Oxidation of 5â€hydroxymethylfurfural into 2, 5â€diformylfuran. Energy Technology, 2017, 5, 1429-1434.	3.8	12
24	Diphyllin Improves High-Fat Diet-Induced Obesity in Mice Through Brown and Beige Adipocytes. Frontiers in Endocrinology, 2020, 11, 592818.	3.5	10
25	Nifedipine di-matrix depot tablets prepared by compression coating for obtaining zero-order release. Drug Development and Industrial Pharmacy, 2018, 44, 1426-1433.	2.0	8
26	Aromatic monoterpenoid glycosides from the seeds of Paeonia ostii. Journal of Asian Natural Products Research, 2017, 19, 1149-1154.	1.4	7
27	Studies on the in vitro ion exchange kinetics and thermodynamics and in vivo pharmacokinetics of the carbinoxamine-resin complex. International Journal of Pharmaceutics, 2020, 588, 119779.	5.2	7
28	Highly Efficient Lightâ€Emitting Diodes Based on an Organic Antimony(III) Halide Hybrid. Angewandte Chemie, 2022, 134, .	2.0	7
29	Enhancement of Glucose Utilization by Loesenerine through AMPK Activation in Myotubes. Chemical and Pharmaceutical Bulletin, 2018, 66, 885-886.	1.3	6
30	The driving effect of substituent size changes on reaction: a novel reaction for direct production of triacetylglycerol from oils and fats. Green Chemistry, 2020, 22, 6345-6350.	9.0	6
31	Antimony-induced astrocyte activation via mitogen-activated protein kinase activation-dependent CREB phosphorylation. Toxicology Letters, 2021, 352, 9-16.	0.8	5
32	Rapid continuous photoflow synthesis of naturally occurring arylnaphthalene lignans and their analogs. Natural Product Research, 2022, 36, 5086-5090.	1.8	3
33	Design of Rational JAK3 Inhibitors Based on the Parent Core Structure of 1,7-Dihydro-Dipyrrolo [2,3-b:3′,2′-e] Pyridine. International Journal of Molecular Sciences, 2022, 23, 5437.	4.1	3
34	Cytotoxic tigliane diterpenoids from Euphorbia neorubella. Natural Product Research, 2021, , 1-5.	1.8	0